

Microzonation of earthquake hazard in Greater Delhi area

R. N. Iyengar* and S. Ghosh

A spate of earthquakes in the recent past, causing extensive damage, has heightened the sensitivity of engineers and planners to the looming seismic risk in densely populated Indian cities. Delhi city is in a seismically active region and hence it is important to understand the existing earthquake hazard to the city on a scientific basis. This article, after discussing the seismo-tectonic status of the city and its environs, presents probabilistic seismic hazard analysis of an area of 30 km × 40 km with its centre at India Gate, Delhi city. The quantified hazard in terms of the rock level peak ground acceleration value is mapped on a grid size of 1 km × 1 km, for a return period of 2500 years. In engineering parlance, this corresponds to a probability of exceedance of 2% in a design life of 50 years. This map can be used as the basis for further site-specific studies at soft soil deposits.

A general review of the seismic status of Delhi, highlighting the importance of seismic microzonation, has been presented earlier¹. Varāha Mihira, who lived in 5–6 century CE, has mentioned northern India, including Delhi and its surroundings as the felt region of severe earthquakes². However, the first historically reported earthquake in Delhi city was on 17 July 1720. The MMI value of this event at Delhi (Old) has been estimated to be IX³. Even though the focus of this event has not been identified, from historical accounts it is surmised that the source should have been in the vicinity of Delhi city. A contemporary account of the high intensity earthquake felt in the Agra–Mathura region on 25 August 1803, has been described by Nazir Akbarabadi (1740–1830) in his Urdu poem *bhūcāl-nāma*⁴. This event caused damage to Qutub Minar, one of the famous landmarks of Delhi. In recent times an event of magnitude $M_L = 6$ occurred on 27 August 1960, having its epicentral tract in the Delhi–Gurgaon region. On 28 July 1994, an event of magnitude $M_L = 4$ caused minor damage to a few old buildings. While these events have had their sources in the Indo-Gangetic plains near Delhi city, distant events originating in the Himalayan plate boundary, such as Uttarakashi ($M_L = 6.4$, 20 October 1991) and Chamoli ($M_L = 6.8$, 29 March 1999) earthquakes have caused non-structural damage in some parts of Delhi. Thus, the hazard at Delhi is controlled broadly by two different tectonic regimes with different recurrence characteristics. The seismic zoning map of India (IS 1893–2002) marks a large region, including Delhi to be in zone IV, specifying thereby the basic peak ground acceleration (PGA) for this region as 0.24 g.

Such a broad zoning is unscientific, because seismic hazard is known to have considerable spatial variability even at shorter wavelengths. Engineering approaches to earthquake-resistant structural design will be successful to the extent that the forces due to future shocks are accurately estimated at the location of a given structure. Moreover, in an ancient city like Delhi, it is not just new constructions that have to be designed to be safe, it is equally important to protect existing monuments, industrial and infrastructure facilities. Earthquakes are low-probability events, but with high levels of risk to the society. Hence, either underestimation or overestimation of seismic hazard will prove costly in the long run. With these points in view, an attempt is made here to prepare a microzonation map of Delhi city and its surroundings using state-of-the-art probabilistic seismic hazard analysis (PSHA) methods.

Seismo-tectonic map

In engineering studies, it is the usual practice to consider a region of 250–300 km around the site for purposes of seismo-tectonic characterization⁵. Here, with India Gate in Delhi as the centre, a circular region of 300 km radius has been assumed as the catchment area for Delhi city. Tectonic features around Delhi city have been previously discussed by Valdiya⁶. This has been further improved here to map all known faults in a radius of 300 km around Delhi city. Twenty faults, movement on which can cause ground vibration at Delhi, are shown in Figure 1. Among these, eighteen faults have been marked following the *Seismo-Tectonic Atlas of India*⁷. A short fault within Delhi city has been identified based on a report of Geological Survey of India (GSI). Sohna fault has been marked based on the work of Srivastava and Roy³. Well-known geological features such as the main boundary fault (MBF) and

The authors are in the Department of Civil Engineering, Indian Institute of Science, Bangalore 560 012, India.

*For correspondence. (e-mail: rni@civil.iisc.ernet.in)

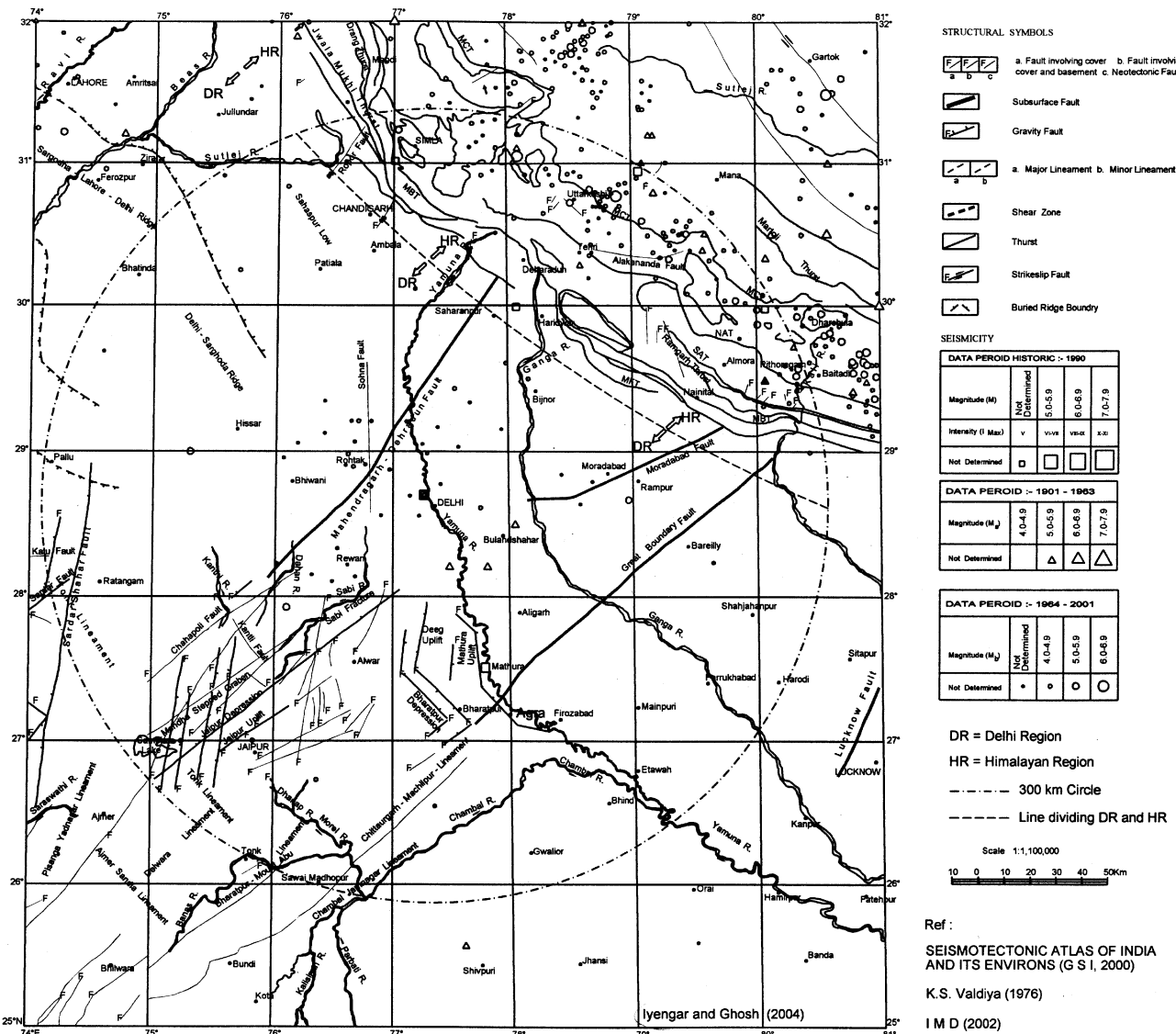


Figure 1. Seismo-tectonic map around Delhi city.

the main crustal thrust (MCT) have several near-parallel tributaries also. In the present study, all such branches have been merged with the parent fault. In Figure 1, the above twenty faults are shown along with the known 278 past epicentres. Figure 1 clearly highlights the susceptibility of Delhi to earthquakes originating either in the Himalayas or from local sources. The faults are numbered for further reference and some details are presented in Table 1. The magnitude M_u given in Table 1 refers to the estimated maximum magnitude that a particular fault may be able to produce. This value has been assigned based on past information, without excessive conservatism. However, this is a point on which further research is needed.

Regional seismicity

The hazard at any point in Delhi is a function of the seismic activity of the region, which in turn is directly related to the individual recurrence property of the listed twenty faults. This amounts to stating that the quantified regional seismicity has to be accounted by the twenty faults in differing proportions. In the present case, this regional seismicity has to be understood for engineering purposes in terms of historical data, in the control region around Delhi city. Here we consider the historical period to be 1720–2001, during which there were 278 catalogued events of $M_L \geq 3$ in the region. Aftershocks of large events have been omitted from this list. It is well known that cata-

logues contain more number of small-magnitude events of recent dates detected with the help of instruments. On the other hand, larger earthquakes are rare but even without instruments their occurrence would be known from general regional history. This points to the limitation that any regional catalogue will be complete, at different magnitude levels, with differing periods of representative history. Quantification of completeness of a catalogue is essential to arrive at reliable (a, b) values in the Gutenberg–Richter recurrence relationship. Here, an additional complication arises due to the control region being not seismically homogenous. To keep the work tractable, with the limited amount of reliable data available, the control region has been divided into two parts denoted as the Himalayan region (HR) and the Delhi region (DR), as shown in Figure 1. The maximum likelihood method proposed by Kijko and Selvola^{8,9}, has been used for each of the two parts, with an upper bound on the maximum magnitude, to obtain the regional (a, b) values. This method can handle small errors and incompleteness in the dataset. This leads to the expected values $b = 0.78$ for HR and $b = 0.87$ for DR. The standard error of b is estimated to be $(b) = 0.04$. The recurrence relationships for the two sub-regions associated with Delhi, are shown in Figure 2.

Fault deaggregation

A given point in the target region will be subject to ground motion from any of the twenty faults. However, each fault has different length, orientation and seismic activity

rate. To compute the ground motion due to an event on a particular fault source s , one needs to know the magnitude of the event and the site-to-source distance. The magnitude of a future event on any fault is a random variable since that fault has a potential to produce an earthquake of magnitude m in the interval (m_0, m_u) according to its own recurrence properties, which are not known. To circumvent this difficulty, the heuristic principle of conservation of seismic activity is invoked. According to this principle, the number of earthquakes per year with $m > m_0$ in the region, denoted as $N_s(m_0)$, should be equal to the sum of number of events $N_s(m_0)$ ($s = 1, 2, \dots, N_s$) possible on the different faults. For PSHA, m_0 can be fixed at 4.0 since events of still lower magnitudes are not of engineering importance. However, any fault longer than the rupture length required to cause an event with $m_0 = 4$, can generate an earthquake in future. This observation leads one to recognize that $N_s(m_0)$ may be taken to be proportional to the length of the fault. This gives the weighting factor $\alpha_s = L_s / \sum L_s$ as an activity indicator for fault s . However, this need not be the only factor influencing $N_s(m_0)$. For example, a shorter fault may be more active at the lower magnitude level m_0 , than a longer fault that is capable of producing a higher magnitude. This property can be included if the slip rate of various faults in the region are known. Since this is not known, one has to proceed differently. All the past earthquakes are assigned to the twenty faults depending on the proximity of the respective epicentres to these faults. This way another weighing factor δ_s , which is the ratio of the past earthquakes attributed to fault s to the total number of earthquakes in the region is obtained. This leads to the relation:

Table 1. Fault characteristics

No.	Fault	M_u	Length (km)	w_s	M_{100}
Delhi region					
1	Great boundary fault	7	320	0.1462	5.18
2	Mahendraghar–Dehradun	7	300	0.2657	5.47
3	Moradabad	6.5	165	0.0790	4.87
4	Chahapoli	5.5	215	0.0872	4.81
5	Sabi Fracture	5.5	195	0.0796	4.78
6	Near Mathura	5	84	0.0371	4.40
7	Parallel fault to no. 6	5.5	115	0.0490	4.59
8	Fault left of Alwar	5	130	0.0547	4.53
9	Fault near Alwar	5	55	0.0260	4.27
10	Fault near Jaipur	5	117	0.0497	4.50
11	Mathura	6	100	0.0432	4.56
12	Sohna	6	105	0.0719	4.80
13	Delhi	4.5	7	0.0106	3.92
Himalayan region					
14	Main Central Thrust	8	350	0.5847	6.87
15	North Almora Thrust	6.9	280	0.1315	6.00
16	Main Boundary Thrust	8	450	0.1647	6.22
17	Alaknanda	5.5	51	0.0454	5.15
18	Ropar	5	35	0.0144	4.61
19	Near Ramgarh	5	37	0.0149	4.62
20	South Almora Thrust	6.5	130	0.0444	5.43

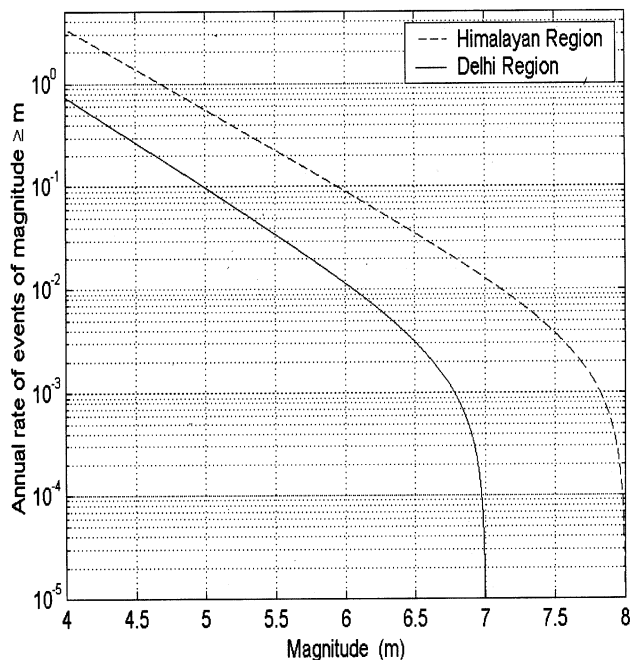


Figure 2. Regional magnitude–frequency relationship.

$$N_s(m_0) = 0.5(\alpha_s + \delta_s) N_r(m_0) \quad (s = 1, 2, \dots, 20). \quad (1)$$

The weight $w_s = 0.5(\alpha_s + \delta_s)$ assigned to each fault is given in Table 1. With the help of eq. (1), the regional recurrence is deaggregated into individual fault recurrence as shown in Figure 3. Here it may be mentioned that the b -value of a fault has been taken to be equal to the regional b -value.

Magnitude uncertainty

For a given site, even when the causative faults are known along with their (a, b) values, the magnitude of a possible future event remains uncertain. However, the magnitude is a random variable distributed between m_0 and m_u following the recurrence relation:

$$\log_{10} N(m) = a - bm. \quad (2)$$

It follows the magnitude random variable M has the probability density function¹⁰:

$$p_M(m) = \frac{\beta e^{-\beta(m-m_0)}}{1 - e^{-\beta(m_u-m_0)}} \quad (m_0 \leq m \leq m_u), \quad \beta = 2.303 b. \quad (3)$$

As an example, the probability density function of possible magnitudes on the Mahendragarh–Dehradun fault is shown in Figure 4.

Uncertainty in hypocentral distance

Another important parameter, which is uncertain, is the source-to-site distance. On an active fault it is possible that all points are equally vulnerable to rupture. Thus, depending on the relative orientation of a fault with respect

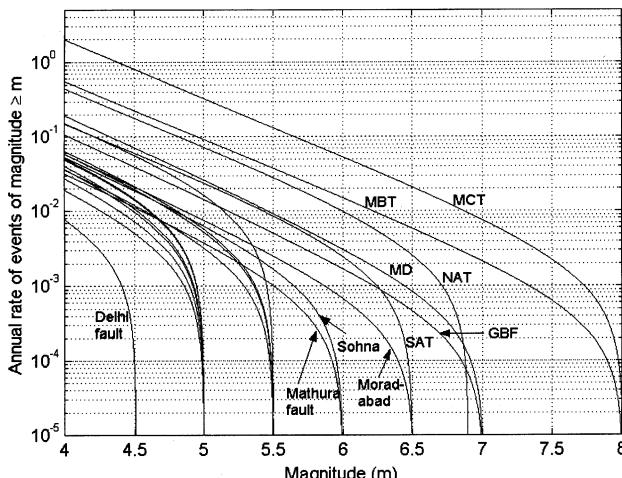


Figure 3. Deaggregation of regional hazard in terms of fault recurrence.

to the station, the hypocentral distance R will have to be treated as a random variable. In the present study, all faults are considered linear with known lengths in the control region (Table 1). Further following Der Kiureghian and Ang¹⁰, the conditional probability distribution function of R given that the magnitude $M = m$ for a rupture segment, uniformly distributed along a fault is given by

$$P(R < r | M = m) = 0 \quad \text{for } R < (D^2 + L_0^2)^{1/2},$$

$$P(R < r | M = m) = \frac{(r^2 - D^2)^{1/2} - L_0}{L - X(m)}$$

for

$$(D^2 + L_0^2)^{1/2} \leq R < \{D^2 + [L + L_0 - X(m)]^2\}^{1/2},$$

$$P(R < r | M = m) = 1 \quad \text{for } R > \{D^2 + [L + L_0 - X(m)]^2\}^{1/2}. \quad (4)$$

Here, $X(m)$ the rupture length in kilometres, for an event of magnitude m is given by

$$X(m) = \text{MIN}[10^{(-2.44 + 0.59m)}, \text{faultlength}]. \quad (5)$$

The notations in eq. (4) are explained in Figure 5. In eq. (5), MIN stands for the minimum of the two arguments inside the parentheses. This condition is used to confine the rupture to the fault length. The first term provides an estimate of the rupture length expected for an event of magnitude m ¹¹. The above solution pertains to the case of

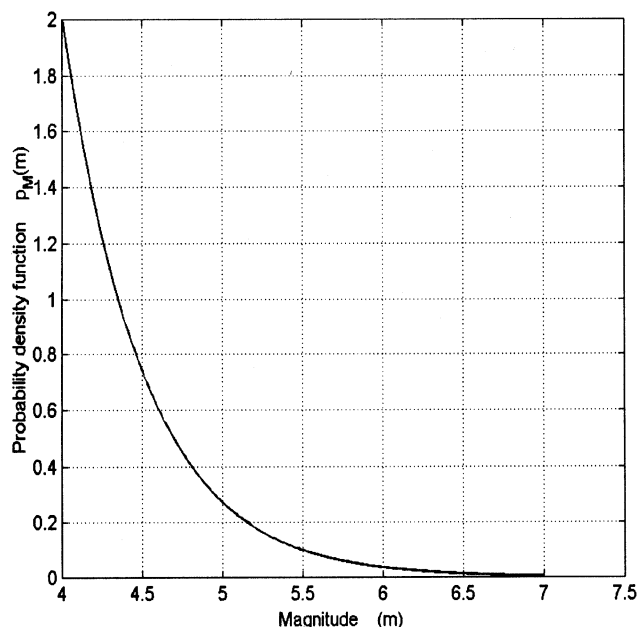


Figure 4. Probability density function of M on the Mahendragarh–Dehradun fault.

a fault situated entirely to one side of a site. In the more general situation when the fault is extending on both sides of the source, the conditional probabilities for the two sides are multiplied by the fraction of length of the corresponding sides and summed up to get the probability for the total fault. As an illustration, the conditional probability density function $p(r|M=6)$ for India Gate with respect to the M-D fault is shown in Figure 6. This function represents all possible distances for an event of $M=6$ occurring on the M-D fault from India Gate.

Attenuation of PGA

The PGA at a site depends strongly on the magnitude of an event and the corresponding hypocentral distance. The pattern of decay of PGA with distance is a property depending on the quality factor appropriate for the region. The current practice is to obtain the attenuation relation by empirical methods, based on instrumental data. For North India, several researchers¹²⁻¹⁴ have worked out such empirical relations. Here, it is noted that the region under consideration overlaps with the region considered by

Sharma¹². However, since Sharma has not reported the standard deviation of the error in the regression, his equation cannot be used in PSHA calculations. Hence, it is thought appropriate to work out a relation valid for rock sites in northern India. By definition, such sites are expected to have a shear wave velocity of $0.76 < V_s < 1.5$ km/s in the top layer of about 30 m. Available strong motion data at such sites consist of 38 samples from Sharma's database plus 23 samples of new data. The resulting attenuation relation valid for rock sites in the Delhi region is obtained as:

$$\log_{10}(y) = C_1 + C_2 M - B \log_{10}(r + e^{C_3 M}) + P\sigma, \quad (6)$$

where $C_1 = -1.5232$, $C_2 = 0.3677$, $C_3 = 0.41$, $B = 1.0047$, $\sigma = 0.2632$. PGA of strong motion records is known to be approximately distributed as a lognormal random variable. Hence, in eq. (6), $P=0$ stands for the median or 50 percentile hazard value. $P=1$ leads to the 84 percentile value of PGA. A comparison between the present equation and the one given by Sharma, for mean PGA value, is shown in Figure 7. The two relations are similar except for minor differences, which are attributable to mixed soil conditions retained by Sharma in his database.

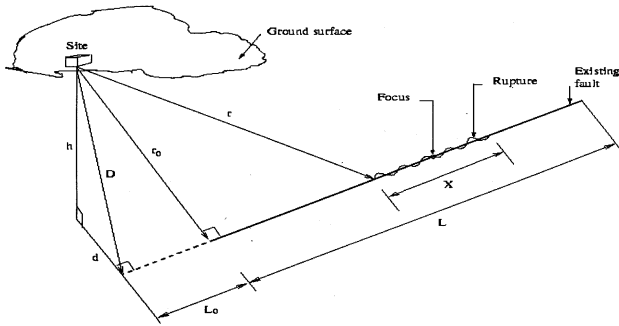


Figure 5. Fault rupture model.

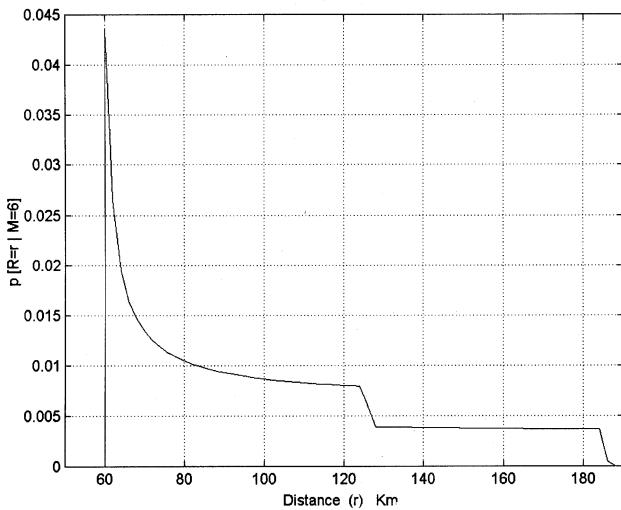


Figure 6. Conditional probability density function of R , $p(r|M=6)$. Site: India Gate; Source: Mahendraghar-Dehradun fault.

Probabilistic seismic hazard analysis

PSHA has been discussed in the literature, notably by Cornell and Merz¹⁵, Der Kiureghian and Ang¹⁰, Bullen and Bolt¹⁶ among several others. Presently, international engineering standards and manuals such as USDOE-1020 (ref. 17), IBC-2003, USNRG-1.165 and EM-1110 (ref. 18) of US Army Corp of Engineers, specify hazard in terms of a given value being exceeded at particular probability levels in a time window of one or more years. If the number of earthquakes on a fault is modelled as a stationary Poisson process, it follows that the probability of the random variable ($Y = \text{PGA}/g$) exceeding the level a in the time period T at a site can be expressed in terms of the annual rate of exceedance μ_a by the equation:

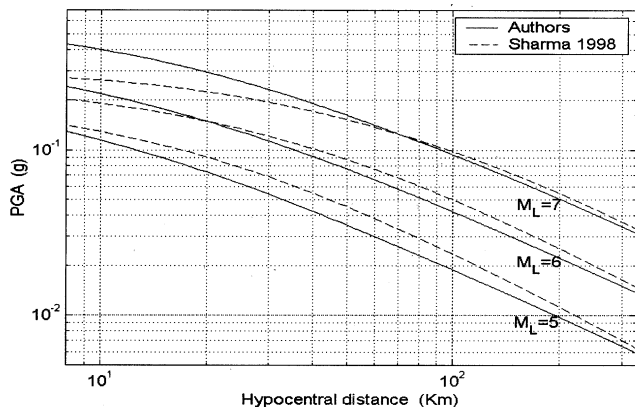


Figure 7. Attenuation of PGA in northern India.

$$P(Y > a) = 1 - \exp(-\mu_a T). \quad (7)$$

The basic expression for μ_a is

$$\mu_a = \sum_{s=1}^{N_s} N_s(m_0) \quad (8)$$

$$\int \int P(Y > a | m, r) p_{R|M}(r | m) p_M(m) dr dm.$$

It is emphasized here that eq. (8) sums up all the individual contributions of twenty faults ($s = 1, 2, \dots, 20$) to obtain the annual probability of exceedance of PGA. As an example, for the central point (India Gate), the individual contribution of all the twenty faults to the mean annual hazard is presented in Figure 8, along with the total value.

Microzonation map

Once the value of μ_a is found at a site, the probability of rock-level PGA exceeding a design value a in a life period of T years is given by eq. (7). By repeating the above computations at various points representing Greater Delhi area, one can construct a hazard microzonation map to any required level of detail. Here, the target region is covered by a rectangular grid of 1320 points at $1 \text{ km} \times 1 \text{ km}$ distance apart. PSHA incorporates all known faults, epicentres, past data and local characteristics in a judicious manner to arrive at site seismic hazard. Here, for Delhi city this has been shown as mean hazard PGA value, with 2% exceedance probability in 50 years. This corresponds nearly to a return period of 2500 years, as suggested by the International Building Code IBC-2003. At the rock level,

it is seen that the hazard peaks up near the local Delhi fault at the centre of the city. This effect is also seen from Figure 8, where the contribution of individual faults to hazard at the centre point has been shown. But, as one moves away from the centre towards the corners, the distance from the Delhi fault increases and its contribution to the hazard decreases. The pattern of the contours in Figure 9 indicates that the hazard is strongly influenced by the southwest-northeast trending M-D fault. The PGA value shown at the centre point of Delhi is of the order of 0.2 g. This value compares with that reported by Khattri¹⁹ at the probability level of 10% for a time window of 50 years. It has to be noted that the results of Figure 9 do not include the effect of soft soil deposits that are widely spread over Delhi. Further refinement of the microzonation map of Figure 9 is to be done by incorporating the effect of soft soil deposits.

Soil conditions

It is well established from past damage surveys that structures on rock behave differently from those founded on soft soil. It is documented that tall buildings with low natural frequencies are vulnerable for greater damage when founded on soft soil deposits²⁰. Delhi is a typical example of a city on the banks of a river that has left several palaeochannels over which presently human settlements exist. Delhi has also rock outcrops in its southern extensions, as seen from Figure 10. Besides the NNE-SSW trending ridge, other parts of the city are overlain with alluvial sediments. These alluvial plains are flat, except for a few interruptions by clusters of sand dunes or rock outcrops. The ridge, which is an extension of the Aravali hills into Delhi, seems to disappear below the western banks of River Yamuna, north of Delhi. The land surface on the eastern side of the ridge is inclined towards River Yamuna

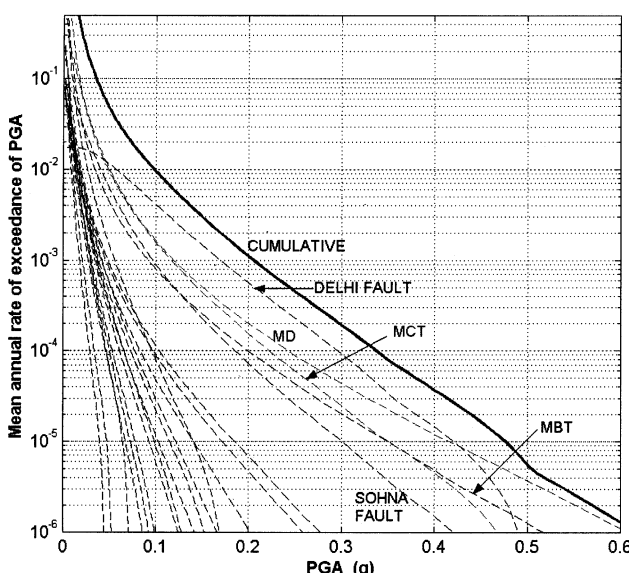


Figure 8. Hazard deaggregation at India Gate due to individual faults.

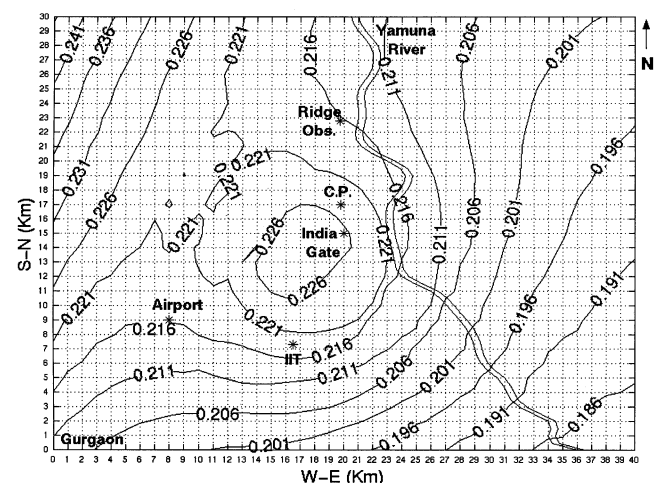


Figure 9. Microzonation of hazard at rock level. Contours of mean horizontal PGA (g) with 2% probability of exceedance in 50 years.

with an average gradient of 3.5 m/km. GSI²¹ summarizes the soil conditions in the metropolitan area in the following manner: 'The depths to bed rock... vary from near surface in Link Road, Pusa Road, Vijay Chowk, Daryaganj areas to as deep as 40 to 60 m in the Patel Road, Lal Quila, Rajghat areas, 80 to 100 m in the Aurobindo Marg–IIT area and 150 m in the Yamuna river bed area. The bedrock topography, in general, is undulating, characterized by several humps and depressions. In the North Delhi area, the depths to bedrock east of the ridge vary from near surface to 30 m, with a gradual easterly slope towards the river Yamuna. West of the ridge in the Mall Road–Imperial Avenue sections, the depths vary from near surface to 30 m and more, with an abrupt deepening to 90 m in the north to as much as 200 m in the Roshanara garden area in the south. In the Sabzi Mandi, Rani–Jhansi Road area the bedrock occurs at shallow depths and at more than 20 m in the Chandni Chowk Sadar Bazar–Lal Quila areas. The bedrock is overlain mostly by clay in the North Delhi, Aurobindo Marg, and Yamuna river bed areas with indications of sand/silt with *kankar* and granular zones at several places. The overlying alluvium east of the ridge appears to be mostly sand/silt with *kankar*'.

Local site effects

The above is a qualitative, large-scale picture of soil conditions in Delhi. Construction sites are small, of the order of a few ten metres. Thus, the local ground vibration transferred to the structure depends sensitively on the detailed vertical make-up of the soils at the site. Hence, a proper study of the effect of local soils on the hazard calls for extensive geo-technical investigations focusing on layering details, their shear-wave velocity and density profiles. Even though in engineering projects bore-hole investigations are common, shear-wave velocities are not routinely measured. Under these circumstances, what has been possible

here is to estimate the fundamental natural frequency of the ground at a few points. At construction sites bore-hole data up to 30–60 m depth are acquired for purposes of foundation design. The geo-technical parameters obtained this way, can be used in understanding how local soils alter the rock-level hazard. Seventeen such bore-hole data from a construction project were acquired by the authors for research purposes. The locations of these data are listed in Table 2 and shown in Figure 10. A typical profile of *N*-value obtained by the Standard Penetration Test (SPT) is shown in Figure 11 to illustrate variation of engineering properties of soils with depth. The *N*-value is widely used as a proxy for shear-wave velocity through empirical correlations. One such relation proposed by Turnbull²² based on Australian and Japanese information is $V_s = 3.9.N + 182.9$ m/s, with a standard error of 70 m/s. In the absence of measured V_s values from Delhi, they have been estimated from reported *N*-values using the above relation (Figure 11). By repeating this exercise for all the seventeen stations, a picture of how V_s varies with depth can be obtained as shown in Figure 12. There is considerable scatter, but one finds the regression equation:

$$V_s = 173 D^{0.2}, \quad (9)$$

where D (in metres) is the average variation. Analytical representation of V_s has practical advantages when a large region overlain with alluvial soils has to be studied. In such a case, the rock-level motion propagates vertically through the soil layers, as in the case of a one-dimensional medium, to arrive at the surface in a modified fashion. This modification, incorporating nonlinear effects and layering properties can be carried out using the standard

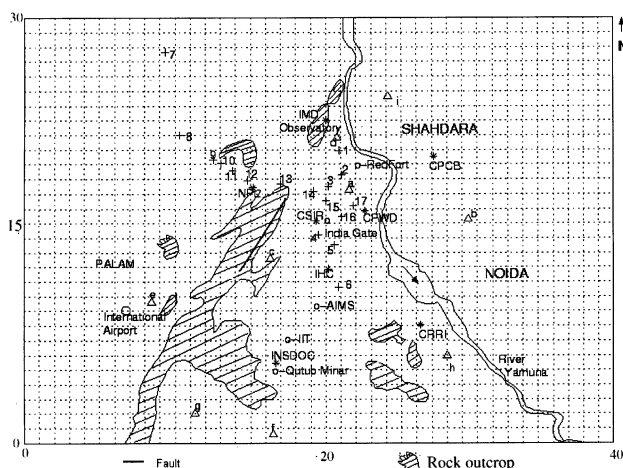


Figure 10. Rock outcrops in Delhi city.

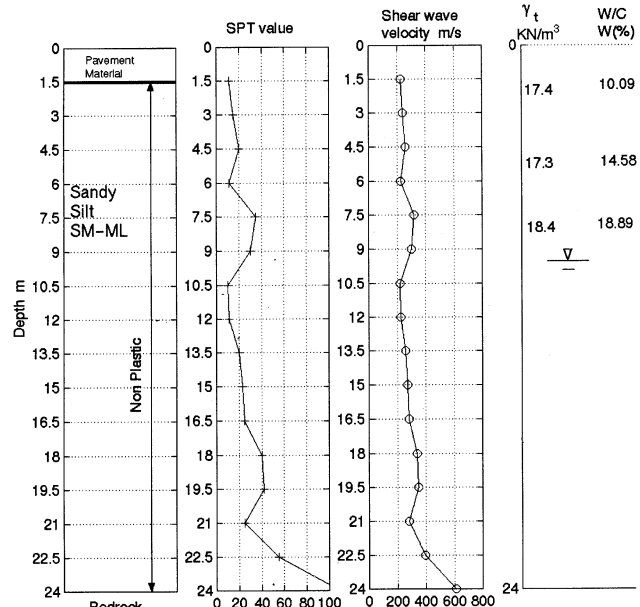
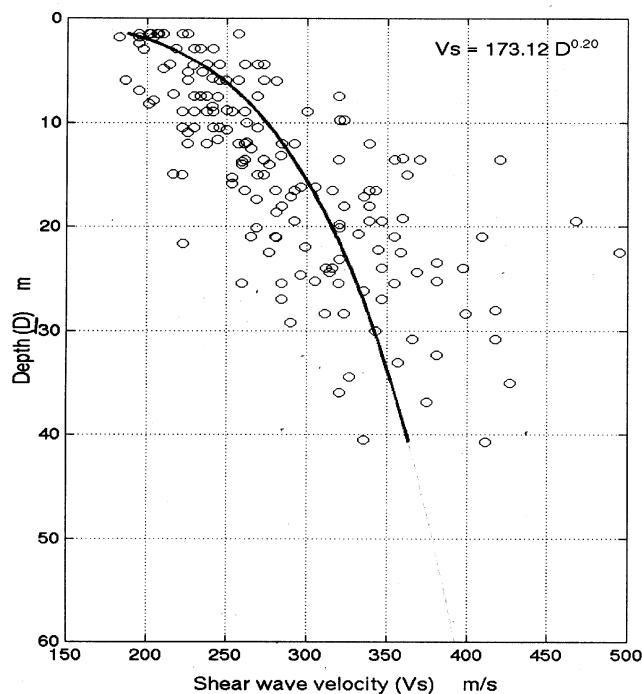


Figure 11. Bore-log at Palika Place.

Table 2. Soil site location and classification (ref. Figure 10)

Site no.	Location	Grid coordinates (km)	No. of layers above rock	Rock depth (m)	Natural frequency (Hz)	V_s^{30} (m/s)	Site class according to IBC-2000
1	Sewanagar	20.9,20.0	10	55	1.00	235	D
2	Shahjahan Road	21.0,18.0	8	32	1.63	270	D
3	Boat Club	20.1,17.5	4	12	5.38	1009	B
4	N.D. Railway Station	19.5,14.2	11	30	1.75	279	D
5	Chawri Bazar	20.6,13.5	4	09	6.00	1130	B
6	ISBT	20.9,10.6	8	30	2.00	317	D
7	Rohini	09.3,27.7	24	200	0.50	269	D
8	Punjabi Bagh	10.3,21.0	18	100	0.75	271	D
9	Kirti Nagar	12.5,19.2	19	40	1.63	318	D
10	Rama Road – Patel Road junction	13.0,19.0	18	27	2.00	296	D
11	Naraina Road – Patel Road junction	13.9,18.5	11	16	2.88	834	C
12	Patel Nagar	14.8,18.0	9	14	2.74	910	B
13	Karol Bagh	17.0,17.5	18	27	1.88	420	C
14	Palika Place	19.2,17.2	16	24	2.13	524	C
15	Connaught Place	20.0,16.5	12	18	2.38	748	C
16	Mandi House	21.0,15.5	11	40	1.88	339	D
17	Tilak Bridge	22.8,16.2	11	40	1.75	257	D

**Figure 12.** Scatter of V_s with depth and variation of mean.

software SHAKE-91 or by other analytical procedures. Here, using the above standard software, the surface amplification function for unit amplitude sinusoidal motion at the rock level is obtained for some stations and presented in Figure 13. The amplification will be maximum corresponding to the natural frequency of the soil deposit. This resonant frequency is plotted in Figure 14, as a function of the depth to rock at the seventeen bore-hole sites.

In Figure 14, natural frequency of a soil deposit with a shear-wave velocity according to eq. (9) is also presented. An interesting conclusion arising out of Figure 14 is that beyond about 100 m, the natural frequency is not sensitive to depth variations. Thus, for engineering purposes, soil investigations have to be carried up to at least 100 m and the material below this may be taken as rock. Another observation is that the natural frequency value given by the smooth curve is not sensitive to layer-by-layer variability in V_s values. In Table 2, the first natural frequency of the local ground is listed along with some layering details. The engineering classification of the sites according to international practice, using the average V_s value in the top 30 m of the soil is also presented in Table 2. It is expected that sites where rock is not too deep would correspond to class B, requiring no corrections. It is seen from Table 2, that this is the case for sites no. 3 and no. 5 with high natural frequencies. At such places, the seismic hazard curve of Figure 9 can be directly used. For other sites, suitable correction for the rock-level PGA value would be necessary. The frequency response functions at C- and D-type sites (Figure 13) indicate that seismic waves in the resonant band of frequencies are susceptible to amplification by factors in the range of 1.5–2.5. Thus, notwithstanding the low PGA values at the rock level, surface acceleration values can be of the order of 0.3 g or more in the Trans-Yamuna region. Engineering properties of soil deposits can vary widely within short distances, particularly near riverbanks. Thus, it will be appropriate to compute surface-level design basis acceleration from rock-level values shown Figure 9, depending on the bore-hole data at the site. Such studies are also indispensable in understanding liquefaction potential of sites with sandy layers.

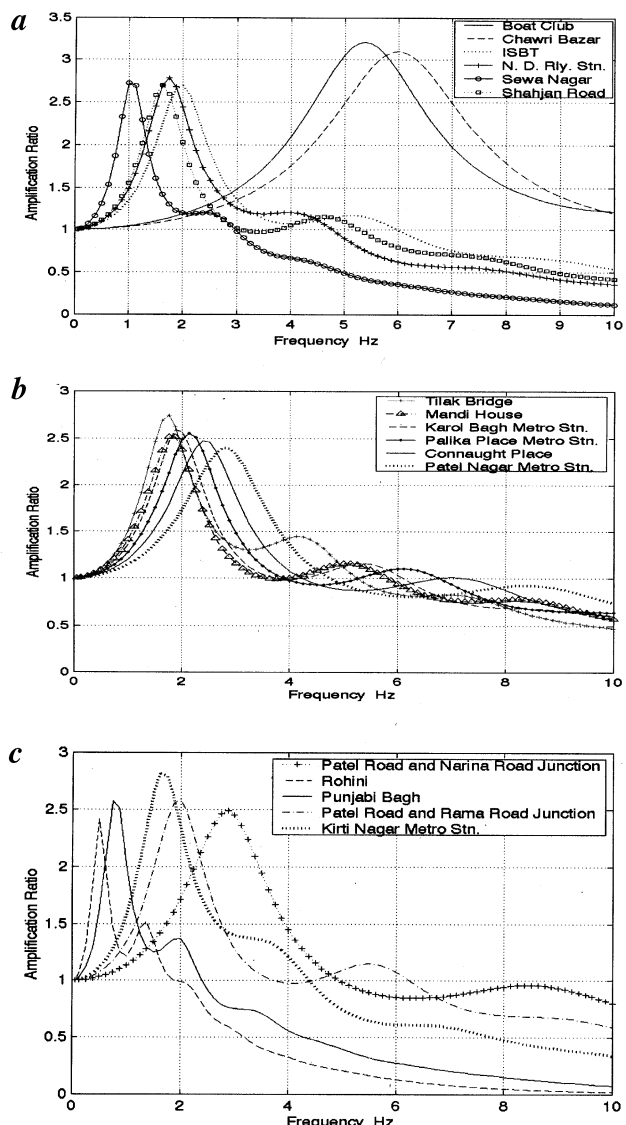


Figure 13a-c. Frequency response functions at the seventeen sites of Table 2.

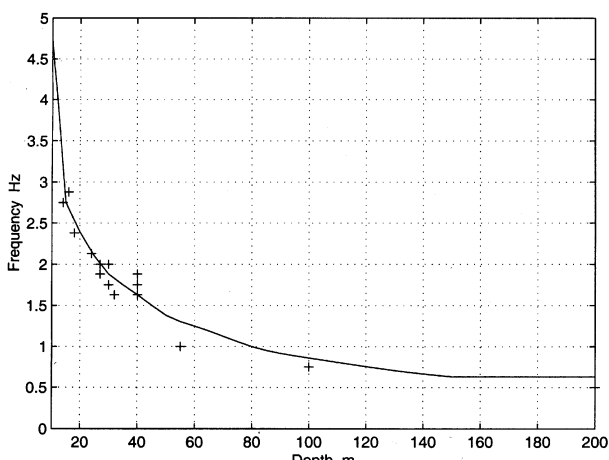


Figure 14. Variation of first natural frequency with depth. (+ +), Layered data; —, With V_s of eq. (9).

Summary and conclusion

Seismic hazard microzonation results for Delhi city are presented. After a review of the seismo-tectonic set-up around Delhi, a controlling region of 300 km radius is considered for detailed study. Regional recurrence relations are obtained based on nearly 300 years of past data. The regional seismicity is distributed essentially among twenty faults of varied lengths and potential. An attenuation relationship valid for the region based on instrumental data on rock sites has been derived. This is similar to the one obtained by Sharma¹² for the same region. Probabilistic seismic hazard analysis has been carried out to arrive at the mean annual probability of exceedance of PGA value at any site. Detailed results are presented in the form of a contour map covering Delhi city and its environs for an extent of 1200 km² on a grid of 1 km². Engineers can use this map directly for rock sites and B-class soil sites in Delhi. For soft-soil sites, further studies are needed to arrive at corresponding surface level PGA values. PSHA carried out here at the rock level is complete, except for data length limitations. However, the soil amplification investigation reported here is only a pilot study. The major limitation has been the non-availability of field measurements for shear-wave velocity in the top layers of the local soils. Nevertheless, the present results form a sound basis for future extensions to cover local soil effects, liquefaction susceptibility, and vulnerability analysis of buildings.

- Iyengar, R. N., Seismic status of Delhi megacity. *Curr. Sci.*, 2000, **78**, 568–574.
- Iyengar, R. N., Earthquakes in ancient India. *Curr. Sci.*, 1999, **77**, 827–829.
- Srivastava, V. K. and Roy, A. K., Seismotectonics and seismic risk study in and around Delhi Region. Proceedings IV Congress International Association of Engineering Geology, New Delhi, 1982, vol. VIII, pp. 77–82.
- UPHS, *Nazir Granthavali: Collection of Poems of Nazir Akbarabadi*, Uttar Pradesh Hindi Sansthan, 1992.
- USNRG, Identification and characterization of seismic sources and determination of SSE ground motion. Regulatory Guide 1.165, 1997, pp. 1–45.
- Valdiya, K. S., Himalayan transverse faults and folds and their parallelism with subsurface structures of north Indian plains. *Tectonophysics*, 1976, **32**, 353–386.
- GSI, *Seismo-tectonic Atlas of India and its Environs*, Geological Survey of India, Kolkata, 2000.
- Kijko, A. and Sellevoll, M. A., Estimation of seismic hazard parameters from incomplete data files. Part I: Utilization of extreme and complete catalogues with different threshold magnitudes. *Bull. Seismol. Soc. Am.*, 1989, **79**, 645–654.
- Kijko, A. and Sellevoll, M. A., Estimation of earthquake hazard parameters from incomplete data files. Part II: Incorporation of magnitude heterogeneity. *Bull. Seismol. Soc. Am.*, 1992, **82**, 120–134.
- Der Kiureghian, A. and Ang, A. H.-S., A fault rupture model for seismic risk analysis. *Bull. Seismol. Soc. Am.*, 1977, **67**, 1173–1194.
- Wells, D. L. and Coppersmith, K. J., New empirical relationships among magnitude, rupture length, rupture width, rupture area, and surface displacement. *Bull. Seismol. Soc. Am.*, 1994, **84**, 974–1002.

12. Sharma, M. L., Attenuation relationship for estimation of peak ground acceleration using data from strong-motion arrays in India. *Bull. Seismol. Soc. Am.*, 1998, **88**, 1063–1069.
13. Jain, S. K., Roshan, A. D., Arlekar, J. N. and Basu, P. C., Empirical attenuation relationships for the Himalayan earthquakes based on Indian strong-motion data. Proc. 6th Int. Conf. on Seismic Zonation, 12–15 November, Palm Spring, CA, USA, 2000.
14. Saini, S., Sharma, M. L. and Mukhopadhyay, S., Strong ground motion empirical attenuation relationship for seismic hazard estimation in Himalayan region. 12th Symposium on Earthquake Engineering, IIT Roorkee, India, 2002, pp. 143–150.
15. Cornell, C. A. and Merz, H. A., Seismic risk analysis of Boston. *J. Struct. Div. ASCE*, 1975, **101**, 2027–2043.
16. Bullen, K. E. and Bolt, B. A., *An Introduction to the Theory of Seismology*, Cambridge University Press, Cambridge, 1985, 4th edn.
17. DOE Std-1020, Natural phenomena hazards design and evaluation criteria for department of energy facilities, US Department of the Energy, Washington DC, USA, 2002.
18. EM 1110-2-6050, Response spectra and seismic analysis for concrete hydraulic structures. *Engineering Manual*, US Army Corps of Engineers, Washington, 1999.
19. Khattri, K. N., Seismic hazard in Indian region. *Curr. Sci.*, 1992, **62**, 109–116.
20. Seed, H. B. and Idriss, I. M., Influence of soil conditions on ground motions during earthquakes. *J. Soil Mech. Found. Div., ASCE (SMI)*, 1970, **94**, 99–137.
21. GSI, *Urban Geology of Delhi*, Miscellaneous Publications, Govt. of India, 1978, 42.
22. Turnbull, M. L., Seismic hazard assessment and microzonation of Bundaberg. Masters Thesis, Central Queensland Univ., Australia, 2001.
23. IMD, Important earthquakes from the IMD catalogue that occurred in the region bounded by 25.5°–31.5°N and 74.5°–80.5°E. Pers. commun., 2002.

ACKNOWLEDGEMENTS. We thank Dr M. Tandon, M/s Tandon Consultants Pvt Ltd, New Delhi for providing borehole data. Help received from Sri S. T. G. Raghukanth in the preparation of the manuscript is acknowledged.

Received 27 May 2004; revised accepted 30 August 2004
